J Physiol 586.17 (2008) pp 4179–4191

Mechanisms by which atrial fibrillation-associated mutations in the S1 domain of KCNQ1 slow deactivation of I_{Ks} channels

Lioara Restier[1], Lan Cheng[1] and Michael C. Sanguinetti

Nora Eccles Harrison Cardiovascular Research & Training Institute and Department of Physiology, University of Utah, Salt Lake City, UT, USA

The slow delayed rectifier K^+ current (I_{Ks}) is a major determinant of action potential repolarization in the heart. I_{Ks} channels are formed by coassembly of pore-forming KCNQ1 α-subunits and ancillary KCNE1 β-subunits. Two gain of function mutations in KCNQ1 subunits (S140G and V141M) have been associated with atrial fibrillation (AF). Previous heterologous expression studies found that both mutations caused I_{Ks} to be instantaneously activated, presumably by preventing channel closure. The purpose of this study was to refine our understanding of the channel gating defects caused by these two mutations located in the S1 domain of KCNQ1. Site-directed mutagenesis was used to replace S140 or V141 with several other natural amino acids. Wild-type and mutant channels were heterologously expressed in *Xenopus* oocytes and channel function was assessed with the two-microelectrode voltage clamp technique. Long intervals between voltage clamp pulses revealed that S140G and V141M KCNQ1-KCNE1 channels are not constitutively active as previously reported, but instead exhibit extremely slow deactivation. The slow component of I_{Ks} deactivation was decreased 62-fold by S140G and 140-fold by the V141M mutation. In addition, the half-point for activation of these mutant I_{Ks} channels was ∼50 mV more negative than wild-type channels. Other substitutions of S140 or V141 in KCNQ1 caused variable shifts in the voltage dependence of activation, but slowed I_{Ks} deactivation to a much lesser extent than the AF-associated mutations. Based on a published structural model of KCNQ1, S140 and V141 are located near E160 in S2 and R237 in S4, two charged residues that could form a salt bridge when the channel is in the open state. In support of this model, mutational exchange of E160 and R237 residues produced a constitutively open channel. Together our findings suggest that altered charge-pair interactions within the voltage sensor module of KCNQ1 subunits may account for slowed I_{Ks} deactivation induced by S140 or V141.

(Received 28 May 2008; accepted after revision 2 July 2008; first published online 3 July 2008)
Corresponding author M. C. Sanguinetti: Nora Eccles Harrison Cardiovascular Research and Training Institute, Department of Physiology, University of Utah, 95 South 2000 East, Salt Lake City, UT 84112, USA.
Email: sanguinetti@cvrti.utah.edu

Atrial fibrillation (AF) affects over 2 million Americans and the number of affected individuals is estimated to increase to > 4 million by 2020 (Go *et al.* 2001). Recent studies have demonstrated that some forms of AF have a genetic basis (Fox *et al.* 2004; Ellinor *et al.* 2005; Arnar *et al.* 2006). Rare monogenic forms of AF are caused by mutations in several K^+ channel subunit genes, including *KCNQ1* (Chen *et al.* 2003*b*; Hong *et al.* 2005; Lundby *et al.* 2007), *HERG* (Sinner *et al.* 2008), *KCNE2* (Yang *et al.* 2004), *KCNJ2* (Xia *et al.* 2005) and *KCNA5* (Olson *et al.* 2006).

KCNQ1 (Kv7.1) α-subunits can coassemble as a homotetramer to form a voltage-gated, delayed rectifier K^+ channel. In the heart, KCNQ1 coassembles with KCNE1 β-subunits to form heteromultimeric channels that conduct the slow delayed rectifier K^+ current, I_{Ks} (Barhanin *et al.* 1996; Sanguinetti *et al.* 1996). Compared to KCNQ1 channel current, I_{Ks} has a markedly slower rate of activation, has a larger unitary channel conductance and does not inactivate (Barhanin *et al.* 1996; Sanguinetti *et al.* 1996; Sesti & Goldstein, 1998; Yang & Sigworth, 1998).

Loss of function mutations in KCNQ1 are the most common cause of inherited long QT syndrome (Wang *et al.* 1996). In contrast, only three gain of function mutations in KCNQ1 have been described, and all cause AF (Chen

L. Restier and L. Cheng contributed equally to the work.

DOI: 10.1113/jphysiol.2008.157511

et al. 2003*b*; Hong *et al.* 2005; Lundby *et al.* 2007). Two of these mutations, S140G (Chen *et al.* 2003*b*) and V141M (Hong *et al.* 2005), are located near the extracellular end of the S1 transmembrane domain, a region not usually considered to have a significant role in gating of voltage-gated potassium (Kv) channels. Indeed, these two mutations have no discernible effects on the gating of homomultimeric KCNQ1 channels. When S140G or V141M KCNQ1 α-subunits are coexpressed with KCNE1 β-subunits, the resulting heteromultimeric I_{Ks} channels appeared to be almost constitutively open (Chen *et al.* 2003*b*; Hong *et al.* 2005). Specifically, outward currents elicited by a step depolarization in voltage clamped cells were characterized by a large instantaneous component and only a small time-dependent component.

Here we used site-directed mutagenesis, functional expression of channels in *Xenopus* oocytes and two-microelectrode voltage clamp techniques to further characterize the functional consequences of the AF-associated mutations (S140G or V141M) in KCNQ1. When long interpulse intervals (100 s) were utilized to elicit I_{Ks}, mutant channels were not constitutively open. Instead, similar to WT I_{Ks}, mutant I_{Ks} channels were initially closed before activating very slowly in response to membrane depolarization. However, mutant S140G and V141M I_{Ks} channels activated at more negative potentials and with a markedly slowed rate of deactivation compared to WT I_{Ks}. Other substitutions of S140 or V141 also slowed I_{Ks} channel deactivation, but not nearly to the same extent as the AF-associated mutations. Thus, the disease-associated mutations S140G and V141M in KCNQ1 are particularly effective at disrupting deactivation of I_{Ks}.

Methods

Molecular biology

Human *KCNQ1* was cloned into the pSP64 oocyte expression vector and 18 mutations of S140 or V141were introduced by site-directed mutagenesis with QuickChange (Stratagene, La Jolla, CA, USA). The presence of the desired mutation and absence of additional changes were verified by restriction mapping and DNA sequencing of the PCR-amplified segment. After transformation, the cDNA was purified using a QIAprep Spin Miniprep Kit (Qiagen, Valencia, CA, USA). Purification of the DNA construct after linearization with *Eco*RI was performed using a QIAquick PCR purification protocol (Qiagen). The cRNA used for oocyte injection was transcribed *in vitro* using SP6 Capscribe (Roche, Indianapolis, IN, USA) or the mMESSAGE mMACHINE SP6 kit (Ambion, Austin, TX, USA). The concentration of the cRNA was quantified with the RiboGreen assay (Invitrogen, Eugene, OR, USA).

Oocyte isolation and cRNA injection

The use of *Xenopus laevis* to harvest oocytes was approved by the University of Utah Institutional Animal Care and Use Committee. Frogs were anaesthetized with 0.2% tricaine methanesulphonate in deionized water before a small abdominal incision was made to remove ovarian lobes. The incision was sutured closed and the frog returned to its aquarium for a recovery period of at least 1 month before the procedure was repeated. After a maximum of three surgical procedures, tricaine-anaesthetized frogs were killed by pithing. Oocytes were manually dispersed from the lobes and the follicle cell layer was removed by treatment for 90–150 min with 1 mg ml^{-1} type II collagenase (Worthington, New York, NY, USA) in ND96 Ca^{2+}-free solution that contained (in mM): 96 NaCl, 2 KCl, 1 $MgCl_2$, 5 Hepes; pH was adjusted to 7.6 with NaOH.

To characterize I_{Ks}, stage IV and V oocytes were coinjected with nearly equimolar amounts of *KCNQ1* and *KCNE1* cRNAs: 6 ng of wild-type (WT) or mutant *KCNQ1* plus 0.6 ng of WT human *KCNE1* cRNA. Oocytes were subsequently stored for 2 days at 18°C in Barth's saline solution that contained (in mM): 88 NaCl, 1 KCl, 0.41 $CaCl_2$, 0.33 $Ca(NO_3)_2$, 1 $MgSO_4$, 2.4 $NaHCO_3$, 10 Hepes, 1 pyruvate plus gentamycin (50 mg l^{-1}); pH adjusted to 7.4 with NaOH.

Two electrode voltage clamp

Oocytes were placed in a 0.2 ml recording chamber and perfused at 1 ml min^{-1} with an external bath solution at room temperature (22–24°C) that contained (in mM): 96 NaCl, 4 KCl, 1 $MgCl_2$, 1 $CaCl_2$ and 5 mM Hepes; pH adjusted to 7.6 with NaOH. Standard two-microelectrode voltage-clamp techniques (Stühmer, 1992) and a GeneClamp 500 amplifier (Molecular Devices, Union City, CA, USA) were used to measure ionic currents from single oocytes. Details of the voltage clamp protocols are described in the figure legends. In general, to record the current–voltage (I–V) relationship for I_{Ks}, oocytes were voltage clamped at a negative holding potential (−90 to −120 mV). Test potential were applied to a variable potential with a fixed incremental increase between successive pulses (e.g. −80 to +60 mV in 20 mV steps). A brief prepulse, applied to the same potential used to measure tail currents, preceded each test pulse. Tail currents were measured upon repolarization of the membrane to a specific return potential as described for each experiment. The interval between test pulses was 20, 100 or 300 s as indicated.

Data analysis

Data acquisition was performed with Clampex 8.2 (Molecular Devices, Union City, CA, USA) and off-line

data analysis was performed with Clampfit 8.2 (Molecular Devices), Origin 7.5 (OriginLab Corp., Northampton, MA, USA), Microsoft Excel and SPSS 12 (SPSS, Inc., Chicago, IL, USA) software.

The voltage dependence of isochronal current activation was estimated by tail current analysis. The tail current amplitude (I_{tail}) was plotted as a function of the test potential (V_t) and the data for individual oocytes fitted with a Boltzmann function. When I_{tail} did not saturate at the most positive V_t, then the maximum I_{tail} was estimated by extrapolation of the Boltzmann function to more positive potentials. Data were normalized to the estimated maximum I_{tail} for each oocyte to obtain a conductance–voltage (G–V) relationship that was fitted with a Boltzmann function:

$$G/G_{max} = 1/\{1 + \exp[-zF/RT(V_t - V_{0.5})]\} \quad (1)$$

where z is the effective valence, F is Faraday's constant, R is the gas constant, T is room temperature in kelvins and $V_{0.5}$ is the potential at which the current is half-activated.

The fitted parameters from the Boltzmann relationships were used to calculate the Gibbs free energy, ΔG_0 (expressed in kcal mol^{-1}) according to:

$$\Delta G_0 = 0.2389 z F V_{0.5} \quad (2)$$

and the mutation-induced changes in ΔG_0 ($\Delta\Delta G_0$), according to:

$$\Delta\Delta G_0 = \Delta G_{0,mutant} - \Delta G_{0,WT} \quad (3)$$

A two-exponential function (eqn (4)) was used to fit the time course of tail currents to determine the fast and slow time constants of current deactivation (τ_f and τ_s):

$$I_{tail}(t) = A_f \exp(-t/\tau_f) + A_s \exp(-t/\tau_s) + C \quad (4)$$

A_f and A_s represent the amplitudes of the fast and slow components of tail current.

All data are expressed as means ± S.E.M. (n = number of oocytes). The comparison between groups was performed using Student's t test and the differences were considered statistical significant for a P-value < 0.05.

Results

S140G and V141M mutations in KCNQ1 slow I_{Ks} deactivation

I_{Ks} channels expressed in *Xenopus* oocytes were activated from a holding potential of −120 mV with 5 s depolarizing pulses applied in 20 mV incremental steps from −120 to +40 mV (Fig. 1*A*). For our initial experiments, the

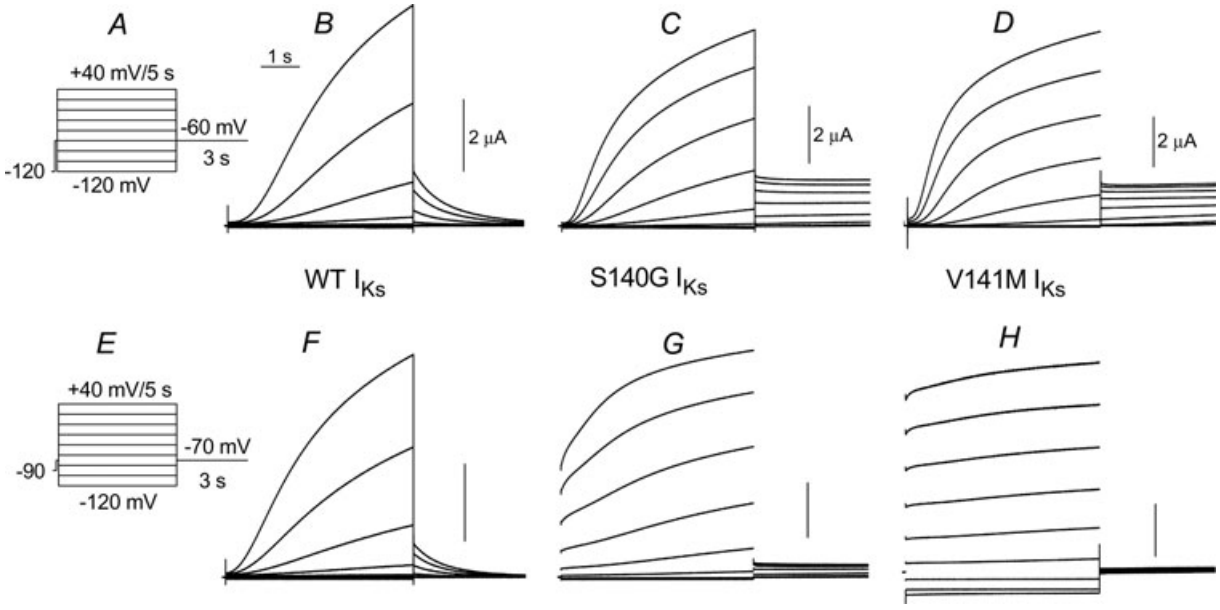

Figure 1. S140G and V141M KCNQ1–KCNE1 (I_{Ks}) channels deactivate very slowly
A, slow voltage pulse protocol used to elicit currents shown in panels *B–D*. From a holding potential of −120 mV, test pulses were applied once every 100 s to potentials ranging from −120 mV to +40 mV. Tail currents were measured at −60 mV. *B–D*, I_{Ks} recorded from *Xenopus* oocytes expressing wild-type (WT), S140G or V141M KCNQ1 α-subunits plus KCNE1 β-subunits. *E*, voltage pulse protocol used to elicit currents shown in panels *F–H*. Test currents were elicited once every 20 s from a holding potential of −90 mV; tail currents were measured at −70 mV. *F–H*, I_{Ks} recorded from the same three oocytes used in panels *B–D*, but using pulse protocol shown in panel *E*. The more rapid pulsing rate prevented complete current deactivation between pulses in oocytes expressing S140G or V141M KCNQ1–KCNE1 channels. The reduced tail current amplitudes for the mutant channels in panels *G* and *H* likely reflects a diminished driving force for K^+ that results from extracellular K^+ accumulation. Capacity transient currents were nulled in all traces. The vertical scale bars represent 2 μA.

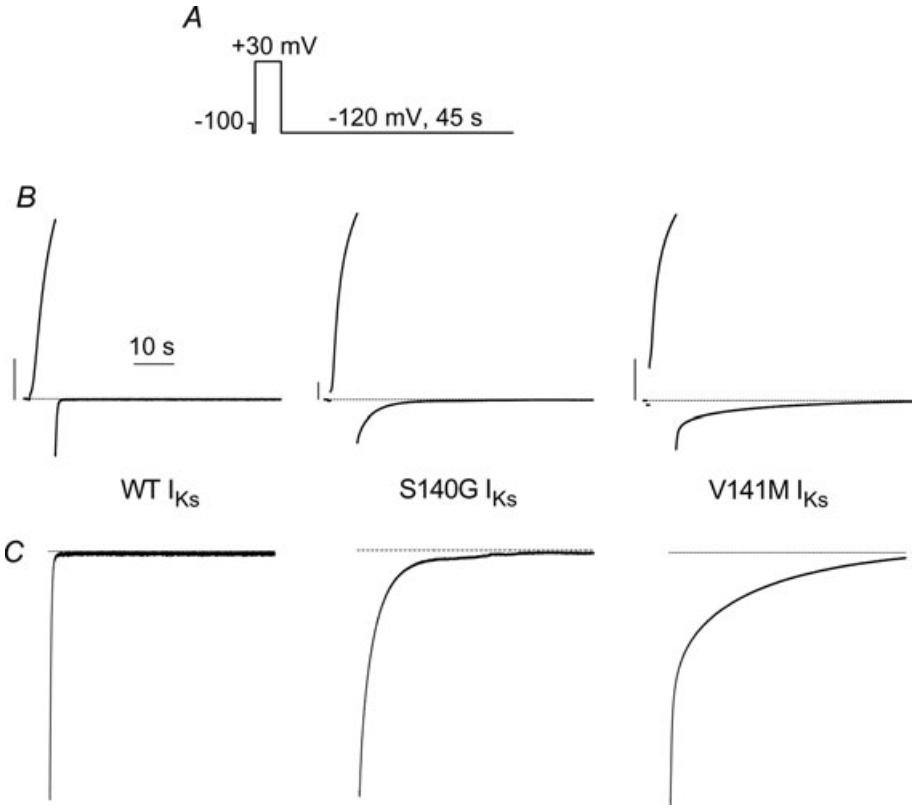

Figure 2. Mutant I_{Ks} channels deactivate slowly at −120 mV
A, voltage pulse protocol. *B*, currents were activated during a 7 s pulse to +30 mV. Deactivating (tail) currents were recorded for 45 s at a return potential of −120 mV. *C*, tail current traces from panel *B* are shown on an expanded *Y*-axis scale.

interpulse interval was set at 100 s to ensure that channels were completely closed between successive test pulses. After each test pulse, the membrane was repolarized to a potential of −60 mV to record deactivating tail currents. Using this pulse protocol, WT I_{Ks} was elicited at test potentials of −20 mV or more positive and activated very slowly. Currents did not reach a steady-state level during the 5 s depolarizing pulses, whereas deactivation at −60 mV was nearly completely after just 3 s (Fig. 1*B*). I_{Ks} conducted by channels formed by S140G KCNQ1

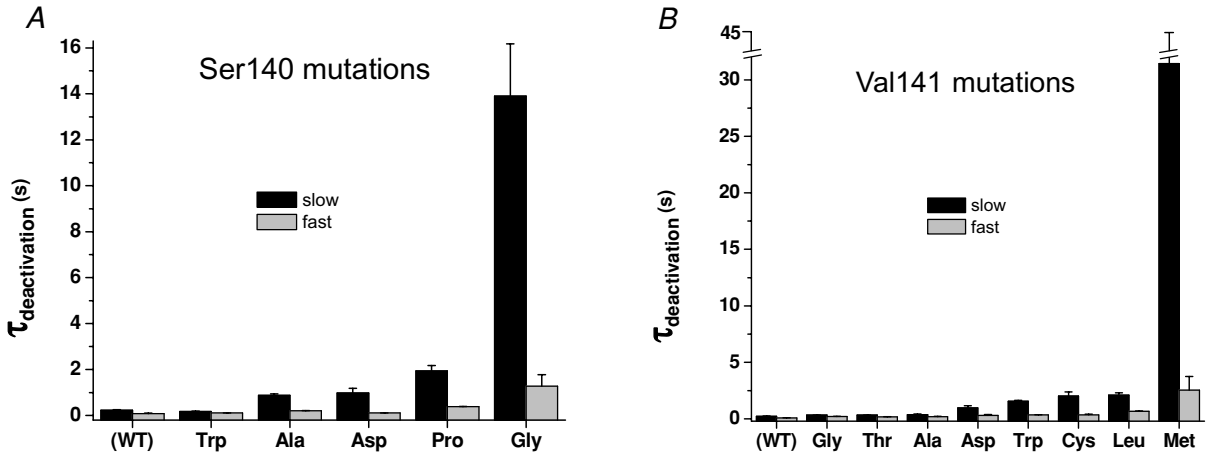

Figure 3. Time constants for deactivation of WT and mutant I_{Ks} channel currents determined at −120 mV
Time constants for fast and slow components of deactivation are plotted for I_{Ks} channels containing mutations of S140 (*A*) or V141 (*B*) ($n = 4$–7).

+ KCNE1 subunits (S140G I_{Ks}) were activated at more negative potentials, with a voltage threshold near −60 mV (Fig. 1*C*). Accounting for the shift in activation, the rate of S140G I_{Ks} was relatively normal; however, tail currents did not deactivate during the 3 s pulse to −60 mV. The kinetics and voltage dependence of I_{Ks} conducted by channels formed by V141M KCNQ1 + KCNE1 subunits (V141M I_{Ks}) was similar to S140G I_{Ks} (Fig. 1*D*). The same oocytes used for these recordings were subjected to another pulse protocol where the holding potential and interpulse interval was altered. For the currents shown in Fig. 1*F–H*, the oocytes were clamped to a less negative holding potential of −90 mV and a shorter interpulse interval of 20 s was used. Test pulses were applied to the same potentials (from −120 to +40 mV), but the tail currents were measured at −70 mV (Fig. 1*E*). The kinetics and voltage dependence of WT I_{Ks} activation was unaltered using this other voltage clamp protocol (Fig. 1*F*). Tail current amplitudes were smaller due to the reduced driving force for K^+ efflux and currents deactivated a little faster because of the more negative return potential. In contrast, S140G I_{Ks} exhibited a prominent instantaneous current component and a reduced time-dependent component during the test pulses (Fig. 1*G*). The relative amplitude of the instantaneous component was even larger for V141M I_{Ks} (Fig. 1*H*). In addition, inward currents were elicited at the test potentials of −100 and −120 mV. Together these experiments demonstrate that the 'instantaneous' currents conducted by mutant I_{Ks} channels, as illustrated in Fig. 1*G* and *H* and reported previously (Chen *et al.* 2003*b*; Hong *et al.* 2005), results from accumulation of channels in the open state when the interpulse interval is too short relative to their markedly slowed rate of deactivation.

The rate of I_{Ks} deactivation for the mutant channels was too slow to accurately quantify at −70 mV. Therefore, we determined the effect of the S140G and V141M mutations on I_{Ks} deactivation at −120 mV (Fig. 2). Currents were activated with a 7 s pulse to +30 mV and deactivating tail currents were measured for 45 s at a return potential of −120 mV. The time required for tail currents to decay at this potential was quantified by fitting the traces to a two-exponential function. The fast and slow time constants (τ_f, τ_s) for deactivation of WT I_{Ks} were 83 ± 18 ms and 224 ± 31 ms ($n = 7$). The S140G mutation increased τ_f and τ_s by 15-fold and 62-fold, respectively (Fig. 3*A*). The V141M mutation slowed deactivation even more, causing a 30-fold and 140-fold increase in τ_f and τ_s, respectively (Fig. 3*B*).

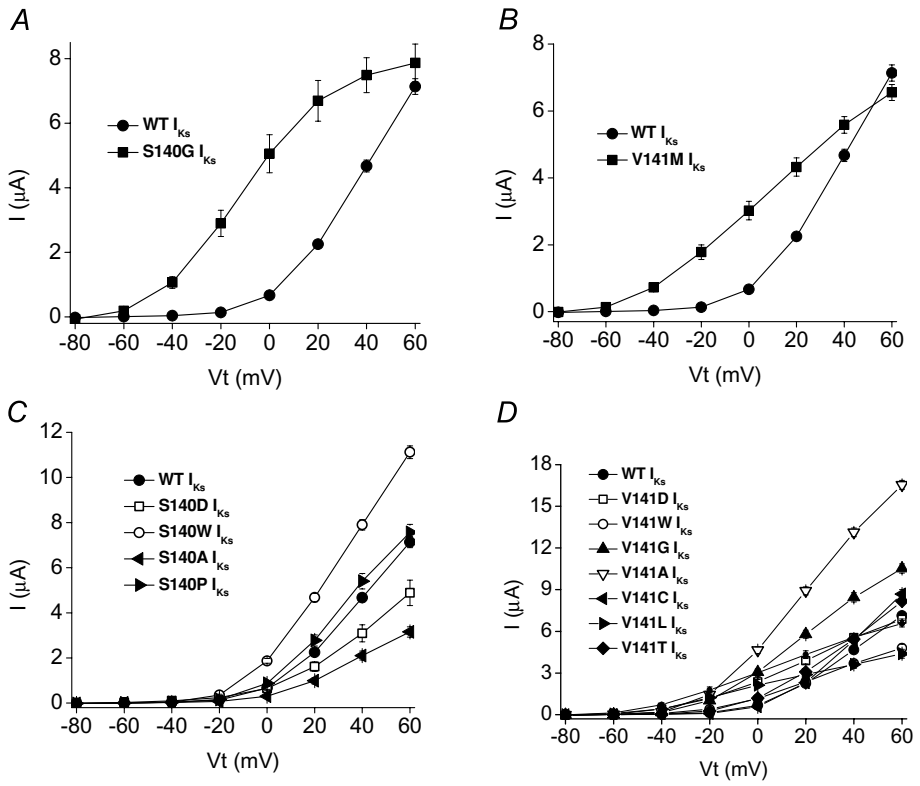

Figure 4
Current–voltage (*I–V*) relationships for WT and mutant I_{Ks} channels. *A* and *B*, *I–V* relationships for WT and S140G or V141M KCNQ1–KCNE1 (I_{Ks}) channel currents as indicated ($n = 6$–10). *C* and *D*, *I–V* relationships for WT and mutant channels carrying the indicated substitutions of S140 and V141 ($n = 6$–10).

Table 1. Voltage dependence of activation for WT and mutant I_{Ks} channel currents

I_{Ks}	n	$V_{0.5}$ (mV)	$\Delta V_{0.5}$* (mV)	z	ΔG_0 (kcal mol^{-1})
WT	10	26.0 ± 0.3	—	1.76 ± 0.09	1.06 ± 0.06
S140G	6	−31.2 ± 0.7†	−57.2	1.87 ± 0.22	−1.34 ± 0.18†
S140W	10	14.4 ± 0.5	−11.6	1.58 ± 0.15	0.52 ± 0.08
S140P	10	22.8 ± 0.4	−3.2	1.77 ± 0.11	0.93 ± 0.07
S140A	8	33.9 ± 0.4	7.8	1.68 ± 0.09	1.31 ± 0.08
S140D	6	35.0 ± 0.5	9	1.26 ± 0.04	1.02 ± 0.05
V141M	7	−27.2 ± 1.5†	−53.2	0.88 ± 0.13‡	−0.55 ± 0.12†
V141L	7	−22.6 ± 1.8†	−48.6	1.05 ± 0.23‡	−0.54 ± 0.17†
V141G	8	0.2 ± 0.3†	−25.8	1.52 ± 0.08	0.01 ± 0.03†
V141A	7	1.8 ± 0.5†	−24.2	1.54 ± 0.12	0.06 ± 0.05†
V141D	7	8.9 ± 0.6†	−17.1	0.83 ± 0.05†	0.17 ± 0.03†
V141W	8	18.9 ± 0.5‡	−7.1	1.17 ± 0.06‡	0.51 ± 0.05‡
V141T	8	24.9 ± 0.8	−1.2	1.33 ± 0.12‡	0.76 ± 0.10
V141C	7	33.4 ± 0.5	7.4	1.71 ± 0.10	1.32 ± 0.10

Half-point ($V_{0.5}$) and effective valence (z) for activation were determined from fitting normalized tail current amplitudes to a Boltzmann function (Fig. 4*C* and *D*). * Shift in $V_{0.5}$ (compared to WT I_{Ks} channels). †$P < 0.002$, ‡$P < 0.05$.

S140G and V141M mutations in KCNQ1 cause a negative shift in the voltage dependence of I_{Ks} activation

The isochronal *I–V* relationship for I_{Ks} was determined using 5 s pulses to potentials ranging from −80 mV to +60 mV and an interpulse interval of 100 s. As noted above, the threshold for activation of S140G I_{Ks} and V141M I_{Ks} was about 40 mV more negative than for WT I_{Ks}. However, when injected with equivalent amounts of *KCNQ1* and *KCNE1* cRNA, the amplitude of I_{Ks} at

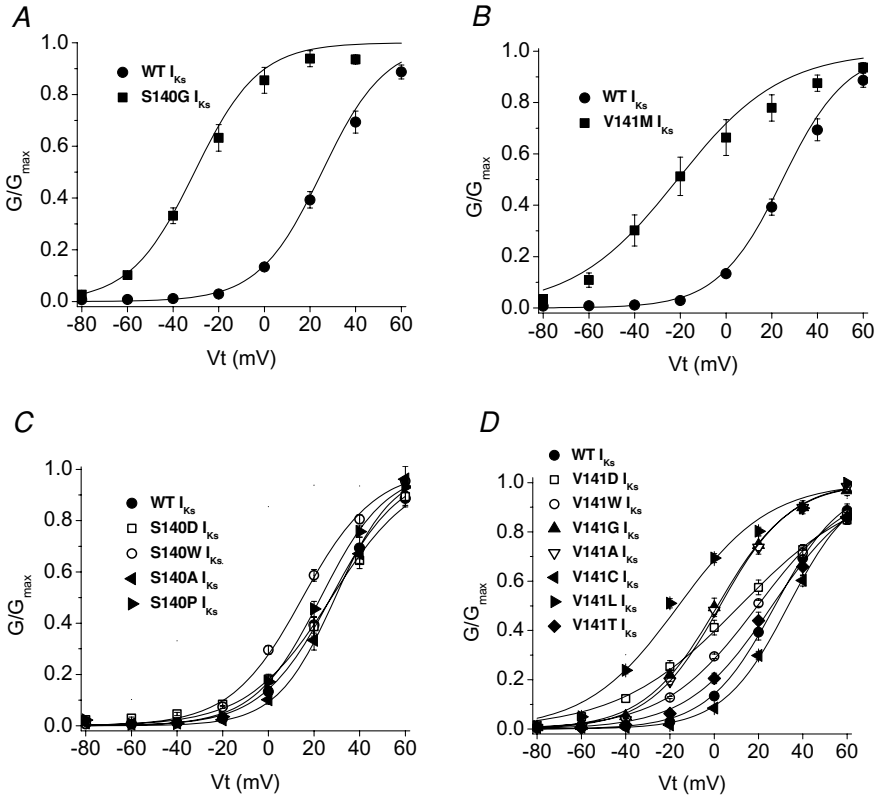

Figure 5. Voltage dependence of activation for WT and mutant I_{Ks} channels
A and *B*, *G–V* relationships for WT, S140G and V141M I_{Ks} channel currents as indicated ($n = 6$–10). *C* and *D*, *G–V* relationships for WT and mutant I_{Ks} channels carrying the indicated substitutions of S140 and V141 ($n = 6$–10). In all panels, data were fitted to a Boltzmann function (smooth curves). Values for $V_{0.5}$ and z are listed in Table 1.

+60 mV was nearly the same for WT and the mutant channels (Fig. 4*A* and *B*).

The voltage dependence of current activation was determined from analysis of peak tail current amplitudes measured at −60 mV. When compared to WT I_{Ks}, S140G and V141M mutations shifted the $V_{0.5}$ by −57 and −53 mV, respectively (Fig. 5*A* and *B*; Table 1). In addition, the slope of the *G–V* relationship for V141M I_{Ks} was shallow compared to WT I_{Ks}.

Other substitutions of S140 and V141 in KCNQ1

The slowed I_{Ks} deactivation induced by S140G or V141M could be a gain of function specific to these mutations. Alternatively, a Ser or Val at these positions could be specifically required for normal I_{Ks} channel function and any mutation of these residues could lead to altered I_{Ks} gating. To discriminate between these two possible mechanisms, we next determined the biophysical properties of channels formed by KCNE1 + KCNQ1 subunits harbouring mutations in S140 or V141 other than Gly or Met.

We mutated S140 to Pro or other residues that were polar (Thr, Cys), hydrophobic (Ala, Met, Trp) or charged (Asp, Arg). Four of the S140 mutations in KCNQ1 (Cys, Met, Arg, Thr) resulted in I_{Ks} amplitudes (~2 μA for 5 s pulses to +60 mV) that were indistinguishable from current induced by injection of oocytes with *KCNE1* cRNA alone, suggesting that these mutations caused a complete loss of KCNQ1 function without a dominant-negative suppression of endogenous KCNQ1 subunits. S140P I_{Ks} was indistinguishable from WT I_{Ks}, whereas S140A and S140D I_{Ks} were smaller and S140W I_{Ks} was larger compared to WT I_{Ks} (Fig. 4*C*). These S140 mutant channel currents had a voltage dependence of activation that was relatively similar to WT I_{Ks} with a $V_{0.5}$ shift < 12 mV (Fig. 5*C*). All mutations except S140W also slowed the rate of current deactivation, albeit not anywhere near the extent observed for S140G (Fig. 3*A*).

We mutated V141 to other residues that were polar (Thr, Cys), hydrophobic (Gly, Ala, Leu, Trp) or charged (Asp). V141L and V141W I_{Ks} were smaller and V141A and V141G I_{Ks} were larger compared to WT I_{Ks} (Fig. 4*D*). Mutation of Val141 to Leu, Gly, Ala and Asp shifted the $V_{0.5}$ for activation to more negative potentials (Fig. 5*D*). The shift induced by V141L was the largest (−49 mV) and was similar to the shift measured for the naturally occurring mutation V141M (−53 mV). All mutations except V141T also slowed the rate of current deactivation, albeit not anywhere near the extent observed for V141M (Fig. 3*B*). Moreover, the slowing of deactivation was not correlated with the shift in $V_{0.5}$ for activation.

The effects of all the S140 and V141 mutations on the voltage dependence of activation, expressed as $\Delta V_{0.5}$ and ΔG_0, are summarized in Table 1. Figure 6 summarizes the effects of all the mutations on I_{Ks} amplitude (measured at +60 mV, Fig. 6*A*) and the mutation-induced change in Gibbs free energy for activation, $\Delta\Delta G_0$ (Fig. 6*B*). All mutations except V141C, V141T, S140D, S140A and S140P decreased $\Delta G_0 > 0.5$ kcal mol^{-1}.

A double mutation (V141M/R237A) in KCNQ1 locks I_{Ks} channels in the open state

R237 is one of three basic residues in the S4 domain of the KCNQ1 subunit that play an important role in voltage

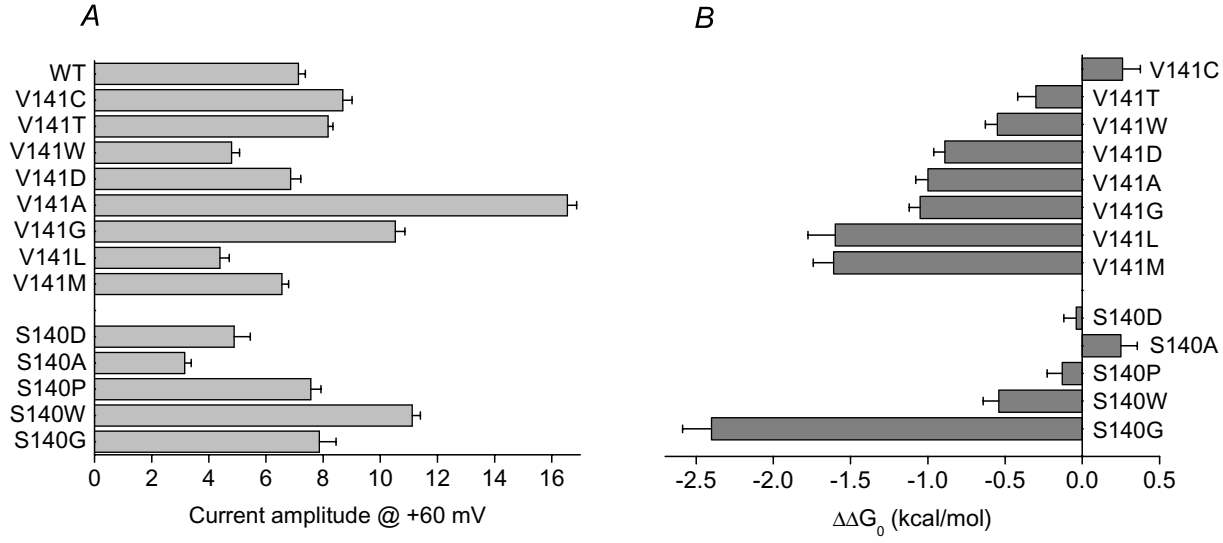

Figure 6. Effects of V141 and S140 mutations on I_{Ks} amplitude and ΔG_0
A, bar graph of I_{Ks} magnitude measured at the end of a 5 s test pulse to +60 mV for WT and mutant channels. *B*, bar graph of mutation-induced changes in ΔG_0 for I_{Ks} channel activation. Number of oocytes (*n*) are reported in Table 1.

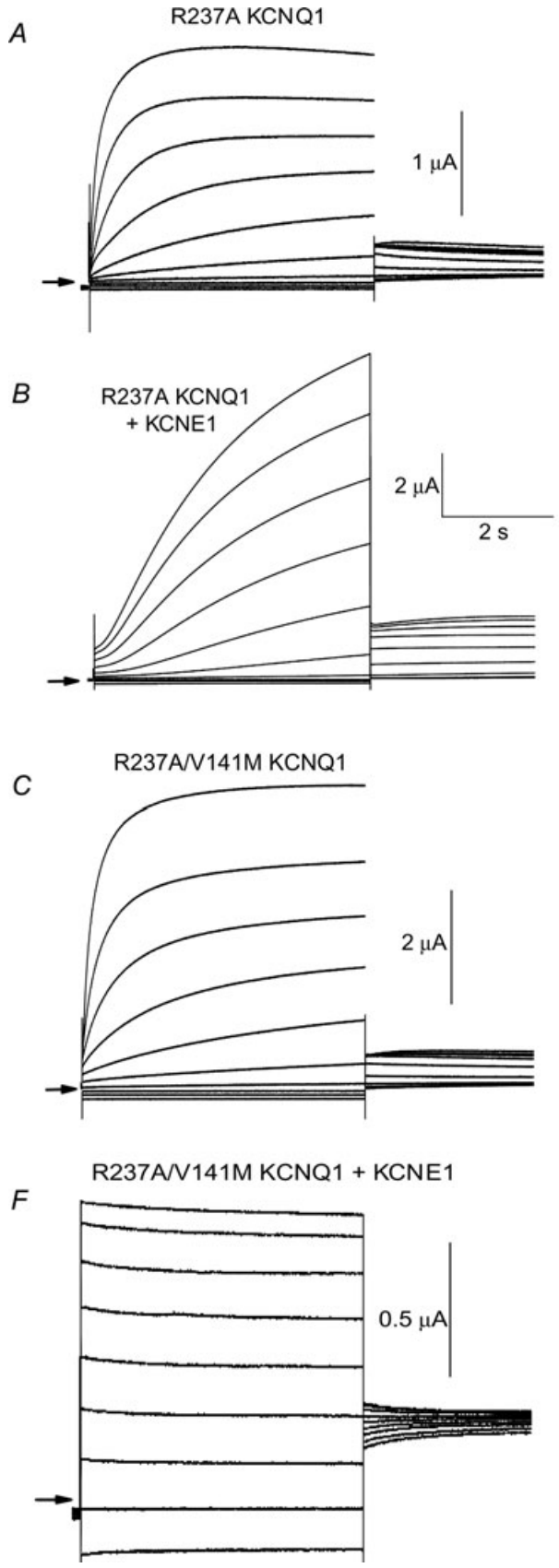

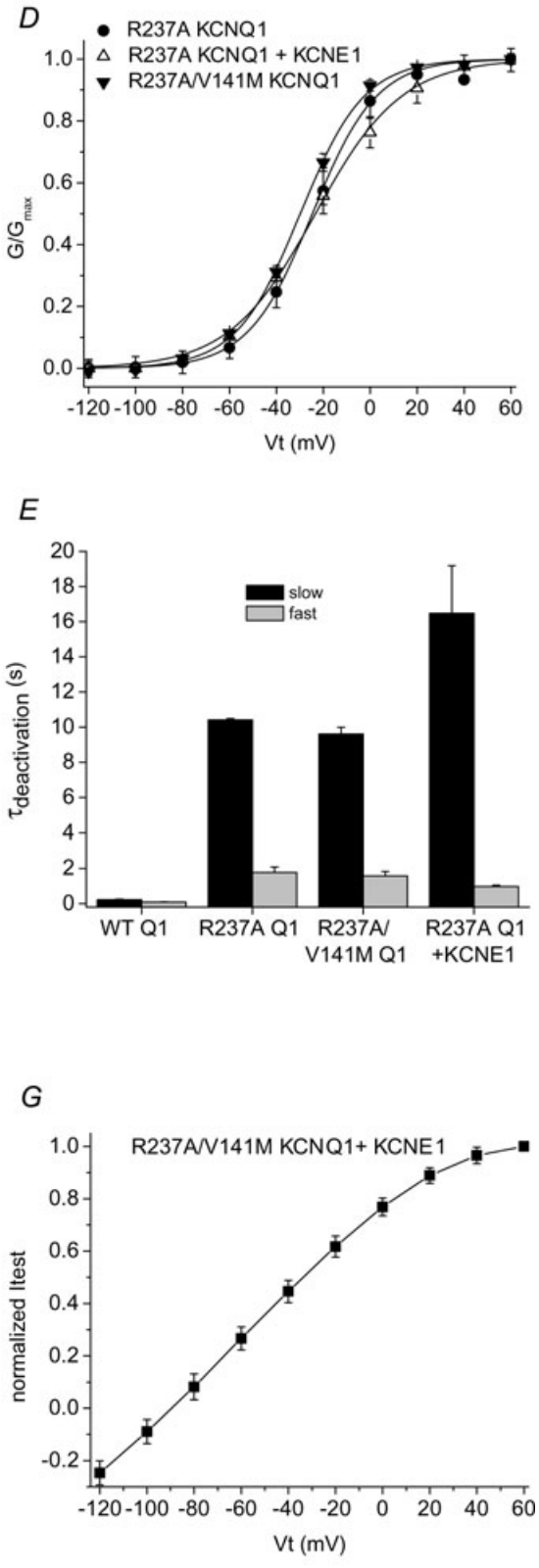

sensing. Recently, Panaghie & Abbott (2007) reported that mutation of R237 to Ala greatly slowed KCNQ1 channel deactivation. Moreover, when coexpressed with KCNE1 subunits, R237A KCNQ1 channels appeared to be constitutively open. We confirmed that R237A KCNQ1 channels deactivated very slowly (Fig. 7*A*). At −120 mV, $\tau_f = 1.8 \pm 0.31$ s and $\tau_s = 10.4 \pm 0.07$ s ($n = 4$). The voltage dependence of activation of this channel was right-shifted by ∼10 mV compared to WT KCNQ1, with a $V_{0.5}$ of -23.0 ± 2.6 mV and a z of 1.53 ± 0.13 ($n = 4$). However, we found that when coexpressed with KCNE1, the resulting R237A I_{Ks} channels were capable of closing if the interpulse interval was sufficiently long; e.g. 90 s (Fig. 7*B*). R237A I_{Ks} channels activated slowly as normal, but deactivation was very slow (at −120 mV, $\tau_f = 0.98 \pm 0.06$ s, $\tau_s = 16.5 \pm 2.7$ s; $n = 7$). In addition, the $V_{0.5}$ for activation of R237A I_{Ks} channels was sifted to more negative potentials ($V_{0.5} = -22.0 \pm 1.5$ mV; $z = 1.24 \pm 0.11$, $n = 7$) compared to WT I_{Ks}, similar to the shift induced by the single mutations S140G and V141M. Thus, in the presence of KCNE1, the R237A mutation in the S4 domain of KCNQ1 mimics the effects of the AF-associated point mutations in the S1 domain. This finding suggested the possibility that the S140G and V141M mutations might alter I_{Ks} gating by interfering with channel gating functions normally subserved by R237. To test this hypothesis, we determined the biophysical properties of channels containing two mutations in KCNQ1: R237A and V141M.

R237A/V141M KCNQ1 channel currents (Fig. 7*C*) had altered biophysical properties similar to that induced by R237A alone (Fig. 7*D* and *E*). This is consistent with our previous findings that V141M alone does not alter gating of KCNQ1 channels (Hong *et al.* 2005). However, R237A/V141M I_{Ks} channels did not deactivate (Fig. 7*F*) and the *I–V* relationship for 5 s test pulses was ohmic between 0 and −120 mV (Fig. 7*G*), even when activated with an interpulse interval of 300 s. Thus, R237A and V141M mutations were synergistic with respect to disruption of I_{Ks} channel deactivation.

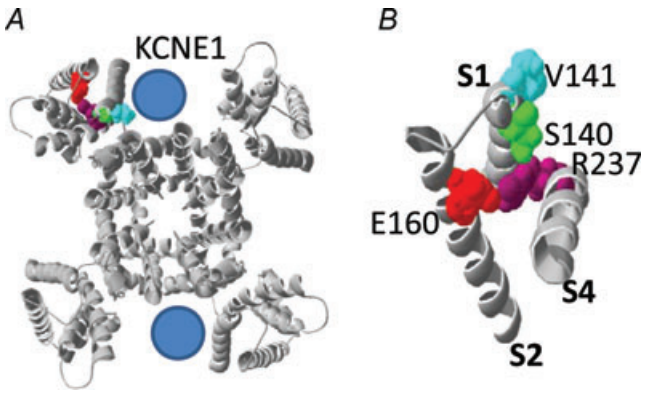

Figure 8. Location of S140 and V141 residues in the KCNQ1 channel
A, entire KCNQ1 channel viewed from extracellular side. In one of the subunits, R237, E160, S140 and V141 are coloured. Location of KCNE1 subunits is speculative. *B*, extracellular view of S1, S2 and S4 segments from a single KCNQ1 subunit. R237 in S4 segment, E160 in S2 segment, and S140 and V141 in S1 segment are labelled. Open state KCNQ1 models modified from Smith *et al.* (2007).

Mutational exchange of two charged residues (E160R/R237E) locks KCNQ1 and I_{Ks} channels in the open state

Smith *et al.* (2007) have proposed a structural model for the closed and open states of the KCNQ1 channel. In this model, mutations in KCNQ1 that cause a gain-of-function of I_{Ks} gating (including S140G and V141M) are located near the outer portion of the crevice proposed to be occupied by a KCNE1 subunit in an I_{Ks} channel. In the closed state, R231 of the S4 segment is adjacent to E160 in the S2 segment, whereas in the open state, rearrangement of the voltage sensor places R237 in close proximity to E160 (Fig. 8). To determine if E160 and R237 interaction is important for KCNQ1 or I_{Ks} channel gating, we swapped the residues at these two positions and examined the effects of single and the double mutations. Channels with the single mutation E160R were non-functional (Fig. 9*A*). E160A KCNQ1 channels were also non-functional (not shown). Channels with the

Figure 7. R237A mutation slows channel deactivation and R237A/V141M I_{Ks} channels are constitutively open
A–C, current traces recorded from *Xenopus* oocytes expressing R237A KCNQ1 alone, R237A KCNQ1 plus KCNE1, or R237A/V141M KCNQ1 subunits. From a holding potential of −100 mV, 5 s test pulses were applied once every 90 s, in 20 mV increments to potentials ranging from −120 mV to +60 mV. Tail currents were measured at −60 mV. Arrows indicate the 0 current level. *D*, voltage dependence of current activation for oocytes expressing the indicated subunits. $V_{0.5}$ and z for *G–V* relationships were as follows: R237A KCNQ1: -23.0 ± 2.6 mV, 1.53 ± 0.13 ($n = 4$); R237A KCNQ1 + KCNE1: -22.0 ± 1.5 mV, 1.24 ± 0.11 ($n = 7$); R237A/V141M KCNQ1: -29.7 ± 1.6 mV, 1.85 ± 0.05 ($n = 5$). *E*, time constants for deactivation determined at −120 mV for WT KCNQ1 (WT Q1, $n = 7$), R237A KCNQ1 ($n = 4$), R237A/V141M KCNQ1 ($n = 5$) and R237A KCNQ1-KCNE1 ($n = 7$) channel currents. *F*, currents recorded from an oocyte expressing R237A/V141M KCNQ1 plus KCNE1 subunits. From a holding potential of −100 mV, 5 s test pulses were applied once every 90 s, in 20 mV increments to potentials ranging from −120 mV to +40 mV. *G*, *I–V* relationship for R237A/V141M I_{Ks} channels ($n = 4$). Currents were normalized to currents at +60 mV.

single mutation R237E activated at much more positive potentials ($V_{0.5} = +42.0 \pm 0.7$ mV, $n = 5$) compared to WT KCNQ1 ($V_{0.5} = -31.5 \pm 1.2$ mV, $n = 6$), but deactivated relatively normally (Fig. 9*B*). Coexpression of R237E KCNQ1 with KCNE1 produced channels with slow activation kinetics typical for I_{Ks} (Fig. 9*C*). In contrast, channels containing both charge-reversing mutations (E160R/R237E) were constitutively open when expressed with or without KCNE1 subunits. Currents were time independent, even when activated with test pulses applied once every 300 s (Fig. 9*D* and *E*). The *G–V* relationships for KCNQ1 or I_{Ks} channels containing the R237E mutation are summarized in Fig. 9*F*. To summarize, the R237E mutation rescued the loss of function induced by E160R and together these mutations prevented channel closure, similar to the phenotype observed for R237A/V141M I_{Ks} channels.

Discussion

Previous studies from Chen *et al.* (2003*b*) and our laboratory (Hong *et al.* 2005) concluded that when coexpressed with KCNE1 β-subunits, S140G or V141M mutations in the S1 domain of KCNQ1 α-subunits caused I_{Ks} channels to be constitutively open. These conclusions were based on experiments where depolarizing pulses were applied at a rate of 6 min^{-1} or faster. Thus, even at very slow physiological heart rates, these mutant channels would be expected to be functionally trapped in their open configuration. In the present study we used extremely slow pulsing (1 pulse every 100 or 300 s) to reveal that these mutant I_{Ks} channels actually can deactivate to a fully closed state, albeit ultra-slowly.

Our experiments used cloned channels expressed in oocytes and currents were recorded at room temperature.

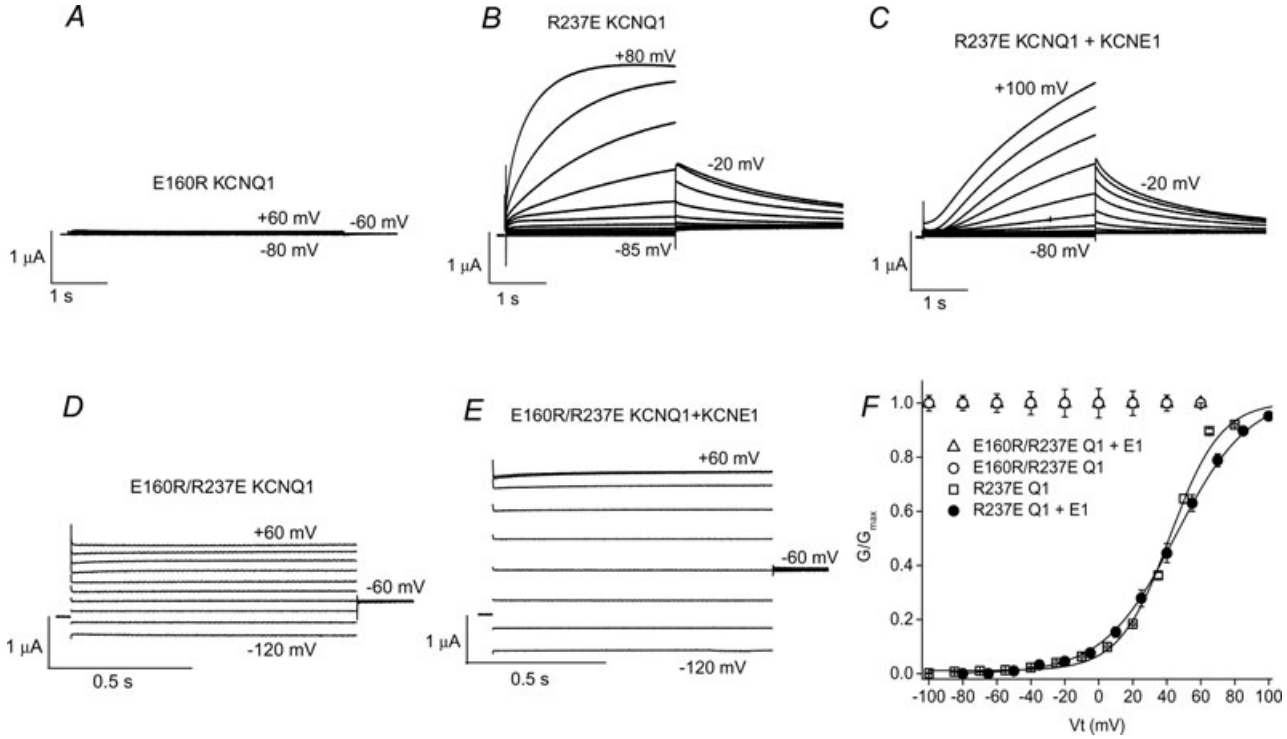

Figure 9. E160R/R237E KCNQ1 and I_{Ks} channels are constitutively open
A, lack of currents recorded in an oocyte injected with E160R *KCNQ1* cRNA. Currents were recorded from a holding potential of −90 mV and 5 s pulses were applied to test potentials ranging from −80 to +60 mV, applied in 20 mV increments. *B*, currents recorded from an oocyte expressing R237E KCNQ1 channel subunits. Holding potential was −90 mV and 3 s pulses were applied to test potentials ranging from −85 to +80 mV, applied in 15 mV increments. Tail currents were measured at −20 mV. *C*, currents recorded from an oocyte expressing R237E KCNQ1 + KCNE1 subunits. Holding potential was −90 mV and 3 s pulses were applied to test potentials ranging from −80 to +100 mV, applied in 15 mV increments. Tail currents were measured at −20 mV. *D* and *E*, currents recorded from oocyte expressing either E160R/R237E KCNQ1 subunits alone (*D*) or with KCNE1 subunits (*E*). currents were recorded from a holding potential of −90 mV and 1 s pulses were applied to test potentials ranging from −120 to +60 mV, applied in 20 mV increments. Tail currents were measured at −60 mV. For panels *A–E*, a few traces are labelled with the corresponding potential (in mV) used to elicit the currents. *F*, *G–V* relationships for oocytes expressing mutant KCNQ1 (Q1) with or without KCNE1 (E1) subunits as indicated. E160R/R237E KCNQ1 + KCNE1 ($n = 6$) and E160R/R237E KCNQ1 ($n = 15$) channels were constitutively open. For R237E KCNQ1 channels, $V_{0.5} = 42.0 \pm 0.7$ mV, $z = 1.91 \pm 0.03$ ($n = 5$). For R237E KCNQ1-KCNE1 channels, $V_{0.5} = 45.1 \pm 2.7$ mV, $z = 1.37 \pm 0.03$ ($n = 7$).

Thus, extrapolation of our findings to the intact human heart has obvious limitations. Nonethelessess, it is clear that the naturally occurring point mutations in S140 and V141 that cause AF (and short QT syndrome for V141M) slowed I_{Ks} channel deactivation more effectively than other substitutions of the native residues. Both mutations shifted the voltage dependence of I_{Ks} gating by about −50 mV. Based solely on this shift in voltage dependence of gating, I_{Ks} deactivation would be expected to be slowed by ∼3-fold (Splawski *et al.* 1997). This is far less than the 62-fold observed for S140G I_{Ks} or 140-fold slowing measured for V141M I_{Ks}, indicating that deactivation was slowed by a mechanism unrelated to the shift in the voltage dependence of activation gating.

Based on multiple lines of evidence, KCNQ1 tetramers can only accommodate two KCNE1 subunits (Chen *et al.* 2003*a*; Morin & Kobertz, 2008). The full range of interactions between KCNQ1 and KCNE1 are uncertain, but previous studies concluded that the α-helical transmembrane domain of KCNE1 associates with the pore region of KCNQ1 (Tai & Goldstein, 1998; Tapper & George, 2000). More recent studies have reported that the α-helical transmembrane domain of a KCNE1 subunit may be positioned in a crevice formed by the intersection of the S1 segment of the voltage sensor domain of one KCNQ1 subunit and the pore domain of an adjacent KCNQ1 subunit (Smith *et al.* 2007; Shamgar *et al.* 2008; Xu *et al.* 2008). Specifically, Xu *et al.* (2008) showed that residue 145 in the S1 domain of KCNQ1 interacts with residues in position 40 and 41 of KCNE1 in a state-specific manner. Situated in this position, it is not difficult to imagine that a KCNE1 protein could influence the coupling between voltage sensing and channel opening to cause slowed channel activation. However, precisely how KCNE1 subunits alter KCNQ1 channel gating is unknown. An equally perplexing question is how S140G or V141M mutations in the S1 domain of KCNQ1 slow deactivation of I_{Ks} in a KCNE1-obligate manner.

Combining the Smith *et al.* (2007) structural model with the functional consequences that result from mutation of charged residues in the voltage sensor module of KCNQ1 and other Kv channels may provide clues into the molecular mechanism for slowed KCNQ1 activation induced by KCNE1 and slowed I_{Ks} deactivation caused by S140G or V141M. One or more salt bridges formed between specific basic residues in S4 and acidic residues in S2 or S3 are required for proper subunit folding and channel assembly of several Kv channels, including *Shaker* (Papazian *et al.* 1995; Tiwari-Woodruff *et al.* 1997; Tiwari-Woodruff *et al.* 2000; Silverman *et al.* 2003), EAG (Silverman *et al.* 2003; Silverman *et al.* 2004), and ERG (Liu *et al.* 2003; Fernandez *et al.* 2005). By analogy, E160 may form a salt bridge with R231 in single KCNQ1 subunits when the channel is in the closed state or with R237 in the open state. The likely importance of E160–R231 interaction for KCNQ1 and I_{Ks} channel assembly and deactivation is supported by our finding that mutation of E160 to Arg or Ala renders the channels non-functional, and that R231A KCNQ1 (Panaghie & Abbott, 2007) and R231W KCNQ1 (Shamgar *et al.* 2008) channels are constitutively open. The loss of function caused by E160R was rescued by the additional charge-reversal mutation R237E. E160R/R237E KCNQ1 channels were constitutively open in the presence or absence of KCNE1, presumably because the ability to form a salt bridge between residues 160 and 237 would be retained in the double mutant channel (favouring the open state), whereas charge repulsion between R231 and R160 would preclude channel closure. Single mutations of R237 were also informative. The R237A mutation markedly slowed KCNQ1 channel deactivation without much affect on the rate or voltage dependence of activation. In contrast, R237E caused a +74 mV shift in the $V_{0.5}$ for KCNQ1 activation, but did not significantly alter the rate of deactivation. Together these findings confirm the importance of R237 in KCNQ1 channel gating (Panaghie & Abbott, 2007) and support the proposal that E160–R237 intrasubunit interactions facilitates activation and stabilizes the open state of KCNQ1 channels. Based on previously published findings and our new mutagenesis results, we suggest that binding of KCNE1 to KCNQ1 subunits slows I_{Ks} channel activation by impeding dissociation of the proposed R231–E160 salt bridge (formed in the closed state) and/or delaying the formation of the R237–E160 salt bridge (formed in the open state).

In the open state model of KCNQ1 (Fig. 8), V141 and S140 in the S1 segment are in close proximity to E160 in S2 and R237 in S4 of the same subunit. The R237A mutation markedly slowed deactivation and thus, mimicked the effect of V141M on I_{Ks}. However, R237A, and not V141M, slowed deactivation of KCNQ1 channels in the absence of KCNE1, indicating that different molecular mechanisms could mediate disruption of channel deactivation by the two mutations. Moreover, combining the two mutations (R237A/V141M) in KCNQ1 produced a synergistic effect, completely preventing the closure of I_{Ks} channels. The S140G and V141M mutations might slow deactivation by interfering with the R231–E160 interaction, or stabilizing the R237–E160 interaction in a KCNE1-dependent manner. Alternatively, S140G and V141M could alter how KCNE1 binds to S1 and thereby disrupt deactivation via an altered interaction between a KCNE1 subunit and the pore domain (S5, S6) of KCNQ1. Obviously, a crystal structure of the I_{Ks} channel would greatly facilitate our understanding of the molecular mechanisms underlying the KCNE1-induced slowing of KCNQ1 activation and the S140G or V141M-induced slowing of I_{Ks} deactivation.

In summary, we report that S140G and V141M I_{Ks} channels retain a capacity to close in a voltage-dependent

manner. Functionally, these mutant channels are constitutively open when activated repetitively at rates that approximate physiological conditions. As described before (Hong *et al.* 2005), these S1 point mutations disrupt I_{Ks} channel gating sufficiently to enhance net outward current during the plateau phase and shorten cardiac action potentials. Finally, we suggest that altered intra-subunit charge-pair interactions between E160 in S2 and R231 and/or R237 of KCNQ1, may account for the slowed I_{Ks} deactivation induced by S140 or V141.

References

Arnar DO, Thorvaldsson S, Manolio TA, Thorgeirsson G, Kristjansson K, Hakonarson H & Stefansson K (2006). Familial aggregation of atrial fibrillation in Iceland. *Eur Heart J* **27**, 708–712.

Barhanin J, Lesage F, Guillemare E, Fink M, Lazdunski M & Romey G (1996). KvLQT1 and IsK (minK) proteins associate to form the I_{Ks} cardiac potassium channel. *Nature* **384**, 78–80.

Chen H, Kim LA, Rajan S, Xu S & Goldstein SA (2003*a*). Charybdotoxin binding in the I_{Ks} pore demonstrates two MinK subunits in each channel complex. *Neuron* **40**, 15–23.

Chen YH, Xu SJ, Bendahhou S, Wang XL, Wang Y, Xu WY, Jin HW, Sun H, Su XY, Zhuang QN, Yang YQ, Li YB, Liu Y, Xu HJ, Li XF, Ma N, Mou CP, Chen Z, Barhanin J & Huang W (2003*b*). KCNQ1 gain-of-function mutation in familial atrial fibrillation. *Science* **299**, 251–254.

Ellinor PT, Yoerger DM, Ruskin JN & MacRae CA (2005). Familial aggregation in lone atrial fibrillation. *Hum Genet* **118**, 179–184.

Fernandez D, Ghanta A, Kinard KI & Sanguinetti MC (2005). Molecular mapping of a site for Cd^{2+}-induced modification of human ether-a-go-go-related gene (hERG) channel activation. *J Physiol* **567**, 737–755.

Fox CS, Parise H, D'Agostino RB Sr, Lloyd-Jones DM, Vasan RS, Wang TJ, Levy D, Wolf PA & Benjamin EJ (2004). Parental atrial fibrillation as a risk factor for atrial fibrillation in offspring. *JAMA* **291**, 2851–2855.

Go AS, Hylek EM, Phillips KA, Chang Y, Henault LE, Selby JV & Singer DE (2001). Prevalence of diagnosed atrial fibrillation in adults: national implications for rhythm management and stroke prevention: the AnTicoagulation and Risk Factors in Atrial Fibrillation (ATRIA) Study. *JAMA* **285**, 2370–2375.

Hong K, Piper DR, Diaz-Valdecantos A, Brugada J, Oliva A, Burashnikov E, Santos-de-Soto J, Grueso-Montero J, Diaz-Enfante E, Brugada P, Sachse F, Sanguinetti MC & Brugada R (2005). De novo KCNQ1 mutation responsible for atrial fibrillation and short QT syndrome in utero. *Cardiovasc Res* **68**, 433–440.

Liu J, Zhang M, Jiang M & Tseng GN (2003). Negative charges in the transmembrane domains of the HERG K channel are involved in the activation- and deactivation-gating processes. *J Gen Physiol* **121**, 599–614.

Lundby A, Ravn LS, Svendsen JH, Olesen SP & Schmitt N (2007). KCNQ1 mutation Q147R is associated with atrial fibrillation and prolonged QT interval. *Heart Rhythm* **4**, 1532–1541.

Morin TJ & Kobertz WR (2008). Counting membrane-embedded KCNE β-subunits in functioning K^+ channel complexes. *Proc Natl Acad Sci U S A* **105**, 1478–1482.

Olson TM, Alekseev AE, Liu XK, Park S, Zingman LV, Bienengraeber M, Sattiraju S, Ballew JD, Jahangir A & Terzic A (2006). Kv1.5 channelopathy due to KCNA5 loss-of-function mutation causes human atrial fibrillation. *Hum Mol Genet* **15**, 2185–2191.

Panaghie G & Abbott GW (2007). The role of S4 charges in voltage-dependent and voltage-independent KCNQ1 potassium channel complexes. *J Gen Physiol* **129**, 121–133.

Papazian DM, Shao XM, Sech S-A, Mock AF, Huang Y & Wainstock DH (1995). Electrostatic interactions of S4 voltage sensor in Shaker K^+ channel. *Neuron* **14**, 1293–1301.

Sanguinetti MC, Curran ME, Zou A, Shen J, Spector PS, Atkinson DL & Keating MT (1996). Coassembly of KvLQT1 and minK (IsK) proteins to form cardiac I_{Ks} potassium channel. *Nature* **384**, 80–83.

Sesti F & Goldstein SA (1998). Single-channel characteristics of wild-type I_{Ks} channels and channels formed with two minK mutants that cause long QT syndrome. *J Gen Physiol* **112**, 651–663.

Shamgar L, Haitin Y, Yisharel I, Malka E, Schottelndreier H, Peretz A, Paas Y & Attali B (2008). KCNE1 constrains the voltage sensor of Kv7.1 K^+ channels. *PLoS ONE* **3**, e1943.

Silverman WR, Bannister JP & Papazian DM (2004). Binding site in Eag voltage sensor accommodates a variety of ions and is accessible in closed channel. *Biophys J* **87**, 3110–3121.

Silverman WR, Roux B & Papazian DM (2003). Structural basis of two-stage voltage-dependent activation in K^+ channels. *Proc Natl Acad Sci U S A* **100**, 2935–2940.

Sinner MF, Pfeufer A, Akyol M, Beckmann BM, Hinterseer M, Wacker A, Perz S, Sauter W, Illig T, Nabauer M, Schmitt C, Wichmann HE, Schomig A, Steinbeck G, Meitinger T & Kaab S (2008). The non-synonymous coding I_{Kr}-channel variant KCNH2-K897T is associated with atrial fibrillation: results from a systematic candidate gene-based analysis of KCNH2 (HERG). *Eur Heart J* **29**, 907–914.

Smith JA, Vanoye CG, George AL Jr, Meiler J & Sanders CR (2007). Structural models for the KCNQ1 voltage-gated potassium channel. *Biochemistry* **46**, 14141–14152.

Splawski I, Tristani-Firouzi M, Lehmann MH, Sanguinetti MC & Keating MT (1997). Mutations in the *hminK* gene cause long QT syndrome and suppress I_{Ks} function. *Nature Genet* **17**, 338–340.

Stühmer W (1992). Electrophysiological recording from *Xenopus* oocytes. *Methods Enzymol* **207**, 319–339.

Tai KK & Goldstein SAN (1998). The conduction pore of a cardiac potassium channel. *Nature* **391**, 605–608.

Tapper AR & George AL Jr (2000). MinK subdomains that mediate modulation of and association with KvLQT1. *J Gen Physiol* **116**, 379–390.

Tiwari-Woodruff SK, Lin MA, Schulteis CT & Papazian DM (2000). Voltage-dependent structural interactions in the *Shaker* K^+ channel. *J Gen Physiol* **115**, 123–138.

Tiwari-Woodruff SK, Schulteis CT, Mock AF & Papazian DM (1997). Electrostatic interactions between transmembrane segments mediate folding of Shaker K^+ channel subunits. *Biophys J* **72**, 1489–1500.

Wang Q, Curran ME, Splawski I, Burn TC, Millholland JM, VanRaay TJ, Shen J, Timothy KW, Vincent GM, de Jager T, Schwartz PJ, Towbin JA, Moss AJ, Atkinson DL, Landes GM, Connors TD & Keating MT (1996). Positional cloning of a novel potassium channel gene: KVLQT1 mutations cause cardiac arrhythmias. *Nat Genet* **12**, 17–23.

Xia M, Jin Q, Bendahhou S, He Y, Larroque MM, Chen Y, Zhou Q, Yang Y, Liu Y, Liu B, Zhu Q, Zhou Y, Lin J, Liang B, Li L, Dong X, Pan Z, Wang R, Wan H, Qiu W, Xu W, Eurlings P & Barhanin J (2005). A Kir2.1 gain-of-function mutation underlies familial atrial fibrillation. *Biochem Biophys Res Commun* **332**, 1012–1019.

Xu X, Jiang M, Hsu KL, Zhang M & Tseng GN (2008). KCNQ1 and KCNE1 in the I_{Ks} channel complex make state-dependent contacts in their extracellular domains. *J Gen Physiol* **131**, 589–603.

Yang Y & Sigworth FJ (1998). Single-channel properties of I_{Ks} potassium channels. *J Gen Physiol* **112**, 665–678.

Yang Y, Xia M, Jin Q, Bendahhou S, Shi J, Chen Y, Liang B, Lin J, Liu Y, Liu B, Zhou Q, Zhang D, Wang R, Ma N, Su X, Niu K, Pei Y, Xu W, Chen Z, Wan H, Cui J & Barhanin J (2004). Identification of a KCNE2 gain-of-function mutation in patients with familial atrial fibrillation. *Am J Hum Genet* **75**, 899–905.

Acknowledgements

We thank Kam Hoe Ng for isolation and cRNA injection of *Xenopus* oocytes. This study was supported by the National Institutes of Health, National Heart Lung and Blood Institute grant number R01 HL065299.